OXFORD

RESEARCH ARTICLE

Large Variation in Brain Exposure of Reference CNS Drugs: a PET Study in Nonhuman Primates

Magnus Schou, Ph.D; Katarina Varnäs, Ph.D; Stefan Lundquist, Ph.D; Ryuji Nakao, Ph.D; Nahid Amini, Ph.D; Akihiro Takano, MD Ph.D; Sjoerd J. Finnema, Ph.D; Christer Halldin, Ph.D and Lars Farde, MD Ph.D

AstraZeneca Translational Science Centre at Karolinska Institutet, Stockholm, Sweden (Drs Schou and Farde); Psychiatry Section, Department of Clinical Neuroscience, Karolinska Institutet, Stockholm, Sweden (Drs Varnäs, Lundquist, Nakao, Amini, Takano, Finnema, and Halldin); AstraZeneca, Innovative Medicines, CNS & Pain, Södertälje, Sweden (Dr Lundquist).

Correspondence: Magnus Schou, PhD, AstraZeneca Translational Science Centre at Karolinska Institutet, Department of Clinical Neuroscience, S-171 76 Stockholm, Sweden (magnus.schou@astrazeneca.com).

Abstract

Background: Positron emission tomography microdosing of radiolabeled drugs allows for noninvasive studies of organ exposure in vivo. The aim of the present study was to examine and compare the brain exposure of 12 commercially available CNS drugs and one non-CNS drug.

Methods: The drugs were radiolabeled with ^{11}C ($t_{1/2}$ = 20.4 minutes) and examined using a high resolution research tomograph. In cynomolgus monkeys, each drug was examined twice. In rhesus monkeys, a first positron emission tomography microdosing measurement was repeated after preadministration with unlabeled drug to examine potential dose-dependent effects on brain exposure. Partition coefficients between brain and plasma (K_p) were calculated by dividing the $AUC_{0-90\ min}$ for brain with that for plasma or by a compartmental analysis (V_T). Unbound K_p ($K_{P\,u,u}$) was obtained by correction for the free fraction in brain and plasma.

Results: After intravenous injection, the maximum radioactivity concentration ($C_{max,\ \%ID}$) in brain ranged from 0.01% to 6.2%. For 10 of the 12 CNS drugs, $C_{max,\ \%ID}$ was >2%, indicating a preferential distribution to brain. A lower $C_{max,\ \%ID}$ was observed for morphine, sulpiride, and verapamil. K_p ranged from 0.002 (sulpiride) to 68 (sertraline) and 7 of 13 drugs had $K_{P\,u,u}$ close to unity. For morphine, sulpiride, and verapamil, $K_{P\,u,u}$ was <0.3, indicating impaired diffusion and/or active efflux. Brain exposure at microdosing agreed with pharmacological dosing conditions for the investigated drugs.

Conclusions: This study represents the largest positron emission tomography study on brain exposure of commercially available CNS drugs in nonhuman primates and may guide interpretation of positron emission tomography microdosing data for novel drug candidates.

Keywords: PET, microdosing, CNS

Introduction

Drug discovery and development has become increasingly challenging, and only a few candidate drugs reach the market. One of the highest attrition rates is in the central nervous system (CNS) therapeutic area, which has been estimated to be >92% (Kola and Landis, 2004). One reason for high attrition is that not all drug candidates cross the blood brain barrier (BBB) to a

sufficient extent to reach pharmacologically relevant concentrations at the target protein, resulting in poor efficacy or low safety margins. To avoid costly attritions in the development phase, it is thus of key importance to confirm brain exposure (commonly referred to as the partition coefficient between drug and plasma) and target engagement at an early stage.

The concept of microdosing refers to studies in which a minute amount of drug is administered and traced in animals or humans to generate early information on pharmacokinetic (PK) properties (Bergstrom et al., 2003; Lee and Farde, 2006; Lappin, 2010). Three different techniques, accelerator mass spectrometry, tandem mass spectrometry, and positron emission tomography (PET), are currently used to perform microdosing studies. Each technique has its different strengths and weaknesses; PET has the distinct advantage of allowing for noninvasive measurements of drug distribution in target tissue. The applications of PET microdosing for brain exposure studies have been reviewed in the literature (Bergstrom et al., 2003; Lee and Farde, 2006), and there is a rich, but inconsistent, literature on PET microdosing studies in nonhuman primates. This lack of consistency, in particular with regard to the methods applied for PET data analysis, prompted us to initiate a more systematic study of PET microdosing for measurements of brain exposure. While this work was in progress, Gunn et al. (2012) applied state of the art methodology for PET data analysis of a PET study in pigs on the brain exposure of a series of investigational drug compounds.

The aim of the present study was to use PET to examine the brain exposure of a set of established CNS drugs to obtain reference values for novel drug developments. Nonhuman primates were used to optimize the predictive validity for humans. The work stream included 4 steps: (1) radiolabel 13 reference drugs, (2) perform nonhuman primate brain PET studies after intravenous injection of a microdose of the radiolabeled drug, (3) use the acquired PET data to calculate parameters relevant to brain exposure, and (4) examine potential dose-dependent effects on brain exposure.

METHODS

Animals and Study Design

The study was approved by the Animal Ethics Committee of the Swedish Animal Welfare Agency (Dnr 145/08, 399/08 and 386/09) and was performed according to the "Guidelines for planning, conducting and documenting experimental research" (Dnr 4820/06-600) of Karolinska Institutet, "Guide for the Care and Use of Laboratory Animals" by Clark et al., the AstraZeneca Bioethical policy, and the EU Directive 2010/63/EU on the protection of animals used for scientific purposes. Five female cynomolgus monkeys (age 5-9 years, weight 4.9-6.2 kg) and 4 female rhesus monkeys (age 7-8 years, weight 5.8-11.6 kg) were supplied by Astrid Fagraeus Laboratory, Karolinska Institutet, Solna, Sweden. Initially, only cynomolgus monkeys were used, but midway through the study, the project gained access to rhesus monkeys, which are larger and enable automated arterial blood sampling. The remaining part of the study was thus conducted in rhesus monkeys.

In cynomolgus monkeys, each of the 13 reference drugs was examined by PET microdosing in 2 monkeys. In the subsequent measurements in rhesus monkeys, each drug was examined twice on the same experimental day, first with a microdose and later with a pharmacological dose in the same monkey.

The 13 reference drugs included in this study were primarily selected on the basis of being established CNS drugs with available PK and pharmacodynamic data (Table 1). To ensure

Table 1. Reference Drugs for PET Microdosing

Reference Drug	Main Pharmacological Target
Caffeine	Adenosine receptor
Citalopram	Serotonin transporter
Clomipramine	Serotonin transporter
Clozapine	Multiple
Diazepam	Gamma-aminobutyric acid receptor
Doxepin	Histamine H1 receptor
Morphine	Opioid receptors
Nicotine	Nicotinic acetyl choline receptor
Seligiline	Monoamine oxidase type B
Sertraline	Serotonin transporter
Sulpiride	Dopamine D2/D3 receptors
Venlafaxine	Serotonin/norepinephrine transporter
Verapamil	Calcium channel

More detailed descriptions of drug properties are provided in table 1 of the supporting information.

facile radiolabeling with carbon-11, only drugs containing methyl groups were selected. Owing to the high specific radioactivity obtained with carbon-11, the average administered chemical dose was 0.17 ± 0.13 µg (mean; SD).

PET Experimental Procedure

Anesthesia was induced by intramuscular injection of ketamine hydrochloride (~15 mg/kg) and, after endotracheal intubation, maintained by a mixture of sevoflurane (1.5%-8%), oxygen, and medical air. The monkey was monitored continuously during the PET experimental days. Body temperature was maintained by Bair Hugger Model 505 (Arizant Healthcare Inc.) and monitored by using an esophageal thermometer. Heart and respiration rates were continuously monitored using the PC-VetGard (TM) system (http://www.vmedtech.com/wireless_monitor.htm). A head fixation system was used to secure a fixed position of the monkey's head throughout the PET measurements undertaken on each experimental day (Karlsson et al., 1993). In each PET measurement, a sterile physiological phosphate buffered (pH 7.4) saline solution containing radiolabeled drug, in a volume not exceeding 5 mL, was injected as a bolus into a sural vein during 5 seconds and PET data acquisition started at time of the bolus injection.

PET measurements were conducted using a High Resolution Research Tomograph (Siemens Molecular Imaging, Knoxville, TN). List mode data were reconstructed using the ordinary Poisson-3D-ordered subset expectation maximization algorithm, with 10 iterations and 16 subsets, including modeling of the point spread function. The corresponding in-plane resolution with an ordinary Poisson-3D-ordered subset expectation maximization point spread function is 1.5 mm in the center of the field of view and 2.4 mm at 10-cm off-center directions (Varrone et al., 2009). Attenuation correction was acquired with a 6-minute transmission measurement using a single ^{137}Cs source. For PET measurements in the initial parts of the study in cynomolgus monkeys, list-mode data were acquired continuously for 93 minutes starting at the time of injection of the radiolabeled drug. Images were then reconstructed for a series of 28 time frames in a sequence consisting of four 30-second frames, four 1-minute frames, eleven 3-minute frames, and nine 6-minute frames. In the later part of the study in rhesus monkeys, PET data were acquired for 123 minutes. Images were reconstructed for a series of 34 frames with a sequence consisting of nine 20-second frames, three 1-minute frames, five 3-minute

frames, and seventeen 6-minute frames. The subsequent quantitative compartmental analysis (see below) was based on PET data acquired between 0 and 90 minutes after injection.

Pharmacological Dosing

In the pharmacological dosing experiments, a solution of the drug in the appropriate vehicle was administered as an infusion (10-20 minutes) that was terminated immediately prior to the admininstration of radiolabeled drug. Caffeine, citalopram, diazepam, doxepine, nicotine, seligiline, sulpiride, and venlafaxine were dissolved in saline. Commercial solutions of clomipramine, morphine, and verapamil were obtained from Apoteket Produktion & Laboratorier AB (Umeå, Sweden). Sertraline was formulated in a 5:3 mixture between phosphate buffered saline and ethanol (30%) in propylene glycol.

Arterial and Venous Blood Sampling

To allow for arterial blood sampling, rhesus monkeys were cannulated in the femoral artery or an artery of the lower limb. To avoid compromising animal health and/or outcome parameters, the aspired blood volume did not exceed 0.7% of the body weight. In addition, saline was used as a volume replacement for the aspired blood. Arterial blood was collected continuously during the first 5 minutes of each PET measurement using an automated blood sampling system (ABSS) (Allogg, Mariefred, Sweden). The ABSS pump speed was set to 3 mL/min. Thereafter, arterial blood samples (1-3 mL) were obtained manually at 5, 8, 15, 30, 45, 60, and 90 minutes after injection. After centrifugation, 0.4 to 2 mL plasma was pipetted and plasma radioactivity was measured in a well counter, consisting of a NaI crystal (Harshaw, diameter 38 mm × 50 mm), a high voltage supply (Canberra, model 3002), an energy discriminator (Canberra, model 818), and a timer and counter (GE&E Ortec, model 871) (Farde et al., 1989). In addition, samples were taken directly from the ABSS at 0.5, 1, 1.5, 2, 2.5, 3.5, and 4.5 minutes for measurement of blood and plasma radioactivity.

Determination of Free Fraction in Plasma

An ultrafiltration method was used to estimate the free (unbound) fraction in plasma ($f_{u \, (plasma)}$). Radiolabeled drug (50 μL) was added to monkey plasma (500 μL) or saline (for control, 500 μL), and the resulting mixture was incubated at room temperature for 10 minutes. After incubation, 200-μL portions of the incubation mixtures were pipetted into ultrafiltration tubes (Centrifree YM-30, molecular weight cutoff, 30 000; Millipore) and centrifuged at 1500 g for 15 minutes. Equal aliquots (20 μL) of ultrafiltrate (C_{free}) and plasma (C_{total}) were measured for their radioactivity with a NaI well-counter. Each determination was performed in duplicate. $f_{u \, (plasma)}$ was calculated as C_{free}/C_{total}, and the results were corrected for the membrane binding measured in control samples.

Determination of Plasma Input Function

The fraction of plasma radioactivity corresponding to unchanged drug in plasma was determined as previously described for PET radioligands (Halldin et al., 2001). Briefly, arterial plasma samples of 1 to 3 mL, sampled at 2.5, 15, 30, 45, 60, and 90 minutes after injection, were deproteinized with acetonitrile and analyzed by gradient high-performance liquid chromatography with radiodetection. The metabolite corrected arterial input function was generated by connecting the ABSS curve with the interpolated curve from the manual blood samples. Corrections for dispersion, plasma radioactivity concentration, and radioactive metabolites were applied to generate the time curve for parent radioactive drug in plasma according to previously described procedures (Farde et al., 1989).

Quantitative Descriptive Analyses

In both cynomolgus and rhesus monkeys, the radioactivity concentration in the region of interest for the whole brain was multiplied with the whole brain region of interest (ROI) volume, divided by the radioactivity injected, and multiplied by 100 to obtain the time curve for the percentage of radioactivity in brain (%ID). Brain and plasma data were also expressed as the standardized uptake value (SUV) corresponding to the regional radioactivity concentration normalized for injected radioactivity and body weight.

The maximum concentration in brain, expressed as the percentage of injected radioactivity ($C_{max, \%ID}$) and as SUV ($C_{max,SUV}$), and the time to the maximum concentration (T_{max}) were determined both for radioactivity in whole brain and metabolite-corrected plasma. The area under the brain as well as the plasma radioactivity concentration-time curve between 0 and 90 minutes after injection ($AUC_{0-90 \, min}$) was calculated by the linear trapezoidal rule. The brain/plasma partition coefficient, that is, the ratio of radiolabeled drug in brain to that in plasma (K_p), was obtained by calculating the ratio between $AUC_{0-90 \, min}$ for brain and plasma or by compartmental analysis (cf. below). In cynomolgus monkeys, no corrections were made for the radioactivity contribution from the cerebral blood due to the absence of arterial blood data.

Compartmental Analysis Using Arterial Input Function

Data for rhesus monkeys were analyzed using the one- (1-TC) and 2-tissue compartment (2-TC) model (Mintun et al., 1984; Huang et al., 1986; Wong et al., 1986) (Figure 1). Time-activity curves for the ^{11}C-labeled drugs in brain were corrected for radioactivity in cerebral blood using the radioactivity concentrations obtained from arterial blood and assuming from the
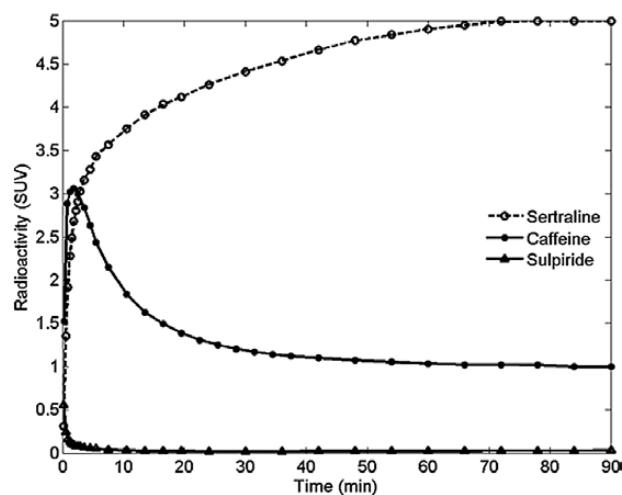

Figure 1. Time curves for brain radioactivity after administration of intravenous microdoses of ^{11}C-labeled sertraline, caffeine, and sulpiride in rhesus monkeys. The time curves were not corrected for radioactivity in cerebral blood.

literature that the cerebral blood volume is 5% of the total brain volume (Farde et al., 1989; Leenders et al., 1990). As the cerebellum is a region having low density of specific binding sites for most of the ^{11}C-labeled drugs investigated, this region was selected in the analyses. Rate constants (K_1 and k_2 in the 1-TC model and K_1, k_2, k_3, and k_4 in the 2-TC model) were determined by curve fitting with a weighted nonlinear least squares fitting technique. K_p, a parameter corresponding to the total volume of distribution (V_T) in the PET literature (Innis and Carson, 2007), was subsequently calculated from the rate constants as follows:

1-TC model:

$$K_P (\text{or VT}) = \frac{K_1}{k_2} \qquad \text{Eq. 1}$$

2-TC model:

$$K_P (\text{or} V_T) = \frac{K_1}{k_2}\left(1 + \frac{k_3}{k_4}\right) \qquad \text{Eq. 2}$$

All kinetic modeling analyses were performed using PMOD v 3.2. The Akaike information criterion (Akaike, 1992) and F-statistics were used to identify the statistically preferred model. Data obtained for the irreversible enzyme inhibitor [^{11}C]selegiline at microdose were in addition analyzed using a 2-TCM with irreversible binding to the second compartment, that is, k_4 was set to zero (Lammertsma et al., 1991).

The free brain/plasma partition coefficient ($C_{u(brain)}/C_{u(plasma)}$ or $K_{P u,u}$) was calculated using the V_T value obtained using PET and in vitro estimates of the fractions of unbound drug in rat brain slices ($V_{u(brain)}$) and nonhuman primate plasma ($f_{u(plasma)}$), according to the following equation:

$$K_{Pu,u} = \frac{V_T}{f_{u(plasma)}V_{u(brain)}} \qquad \text{Eq. 3}$$

$K_{P u,u}$ or $C_{u(brain)}/C_{u(plasma)}$ can also be calculated using the following equation:

$$\frac{C_{u(brain)}}{C_{u(plasma)}} = \frac{f_{u(brain)}K_P}{f_{u(plasma)}}, \qquad \text{Eq. 4}$$

where $f_{u(brain)}$ and $f_{u(plasma)}$ are the fractions of unbound drug in brain tissue and plasma, respectively. The fraction $f_{u(brain)}$ (from homogenate) was obtained from in vitro values reported in the literature (Maurer et al., 2005; Kalvass et al., 2007; Summerfield et al., 2007; Rollema et al., 2010; Di et al., 2011), as were values for $V_{u(brain)}$ (from brain slices) (Friden et al., 2011).

Results

All 13 drugs were radiolabeled and examined in cynomolgus and rhesus monkeys. All monkeys were examined according to the protocol.

PET Examination of Brain Exposure in Cynomolgus Monkeys

The shape of the time-radioactivity curves for brain differed substantially between the tested drugs (Figure 1). For instance, the T_{max} ranged between 0.75 minute for caffeine to 102 minutes for sertraline (supplementary Table 2), whereas selegiline, an irreversible enzyme inhibitor (Fowler et al., 1987), did not reach C_{max} during the PET measurement.

Among the reference drugs, brain $C_{max, \%ID}$ (Figures 2 and 3; supplementary Table 2) varied almost 6-fold between the drugs, from 1.1% for morphine to 6.2% for nicotine. The corresponding $C_{max, SUV}$ ranged between 1.0 and 5.7. A similarly low C_{max} as that observed for morphine was also observed for verapamil, a known substrate for the BBB transport protein PgP, as well as for sulpiride. For the remaining 10 investigated drugs, the $C_{max, \%ID}$ ($C_{max, SUV}$) values were >2.0% (1.8 SUV) (Table 2).

Importantly, the C_{max} values for cynomolgus monkeys were obtained without correction for radioactivity in cerebral blood, since it was not possible to obtain an arterial blood curve. To overcome this limitation, the next series of PET measurements were run in rhesus monkeys.

PET Examination of Brain Exposure in Rhesus Monkeys

Correction for radioactivity in cerebral blood had the greatest effects on sulpiride and morphine, for which almost all radioactivity measured in brain by PET originated from blood (Tables 2 and 3). The seemingly high interspecies variability for some drugs can thus almost entirely be ascribed to this difference in applied methodology. $C_{max,\%ID}$ ($C_{max,SUV}$) in rhesus monkeys ranged from practically negligible (0.01% [0.01SUV]) for sulpiride to 6.2% (5.5 SUV) for clomipramine. Notably, after correction for vertebral blood, the C_{max} for the PgP substrate verapamil was greater than for both morphine and sulpiride. For the remaining 10 investigated drugs, a $C_{max,\%ID}$ ($C_{max,SUV}$) >2.2%ID (2.0 SUV) was obtained.

The partition coefficients between drug in brain and plasma (AUC_{brain}/AUC_{plasma}, K_P) obtained at microdosing conditions in rhesus monkeys ranged from 0.002 for sulpiride to 25.5 for doxepin (Table 2). Unbound partition coefficients, obtained by
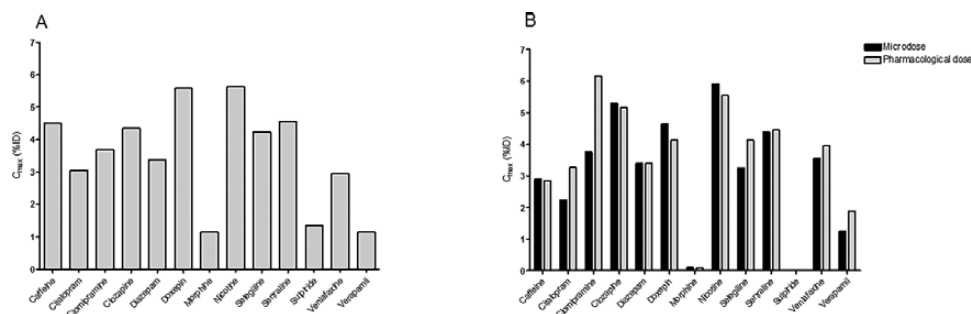

Figure 2. C_{max} in brain measured with positron emission tomography (PET) after intravenous injection of microdoses of radiolabeled drugs in (A) cynomolgus monkeys (mean of 2 measurements) and (B) rhesus monkeys. A PET measurement after pharmacological dosing followed the PET microdosing measurement in rhesus monkeys.
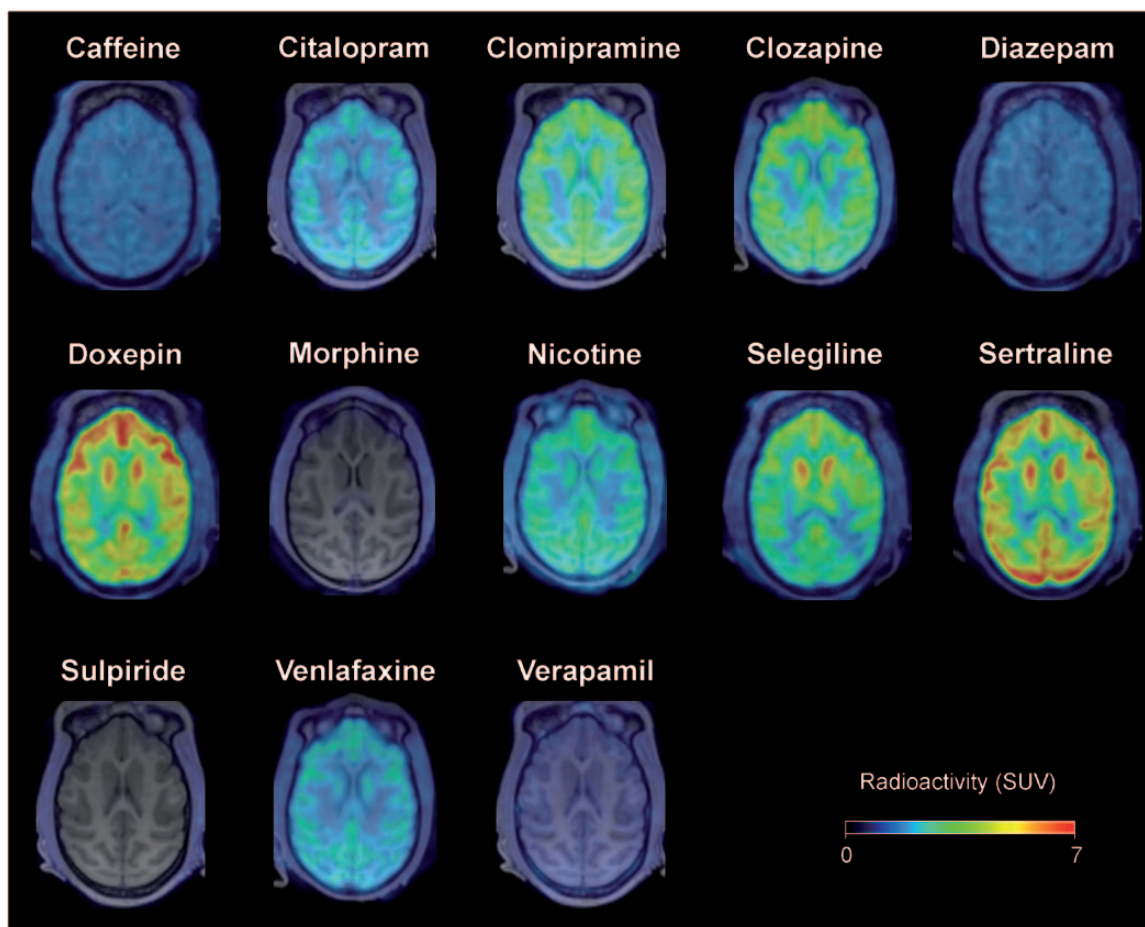
Figure 3. Color-coded summation brain positron emission tomography (PET) images obtained for the time period between 3 and 93 minutes after injection of a series of radiolabeled commercially available drugs.

correcting K_p with unbound fractions of drug in brain (estimated from homogenates) and plasma (measured by ultrafiltration), ranged from 0.001 for sulpiride to 12.1 for clomipramine. When instead using the literature estimates for unbound fraction of drug in brain obtained from brain slices, the range for unbound partition coefficients was between 0.001 for sulpiride and 2.3 for clomipramine (Table 2).

K_p obtained by compartmental analysis of the PET data (V_T values) ranged between 2.8 for verapamil and 68 for sertraline. The compartmental analysis failed to converge for morphine and sulpiride due to the low brain exposure of these drugs. K_p-estimates obtained using the AUC ratio method were systematically lower than those obtained by compartmental analysis (supplementary Table 3). $K_{p\ u,u}$-values were closer, or close to, unity after correcting for free fractions in brain and in plasma ($K_{p\ u,u}$) (Tables 2 and 3), in particular when using the estimated values for unbound fraction in brain reported for brain slices.

Microdoses vs Pharmacological Doses

In general, the PK parameters and variables measured at microdosing conditions were not markedly different at pharmacological drug dosing (Tables 2 and 3, Figure 4). The largest difference between the 2 conditions was observed for T_{max}, which was on average 1.5-fold longer at microdosing conditions. V_T was the second most affected parameter, on average showing a 1.3-fold decrease between microdosing and pharmacological dosing

conditions. The C_{max} in brain obtained at pharmacological dosing conditions was on average 1.1-fold higher than under microdosing conditions.

Drug Metabolism

The metabolism of radiolabeled drugs was assessed in nonhuman primate plasma in parallel with the PET measurements to generate an arterial input function corrected for radiometabolites. Differences in drug metabolism between microdosing and pharmacological dosing were generally small (supplementary Table 4).

PK Modeling

For the majority of drugs studied, the 2-TC model was statistically preferred over the 1-TC model (Table 3). Exceptions were clomipramine and sertraline at both doses, and citalopram, clozapine, and doxepin data obtained after administration of a pharmacologic dose, for which the 1-TC model was sufficient to describe the data. The selegiline PET data at microdose could be described by the 2-TC model with irreversible binding to the second compartment (Lammertsma et al., 1991).

Discussion

The present PET study in nonhuman primates represents the largest examination of the brain exposure of a series of

Table 2. Pharmacokinetic Parameters for Intravenously Injected Microdoses of [11C]-Labeled Drugs in Rhesus Monkeys

Drug	Dose (mg/kg)	$C_{max,\%ID}$ brain (%ID)	$C_{max,SUV}$ brain (SUV)	T_{max} brain (min)	$f_{u(plasma)}$	$f_{u(brain)}$	$V_{u(brain)}$	$\dfrac{AUC_{brain\,0\text{-}90min}}{AUC_{plasma\,0\text{-}90min}}$ (K_P)	$\dfrac{f_{u(brain)}/f_{u(plasma)}\,AUC_{brain\,0\text{-}90min}}{AUC_{plasma\,0\text{-}90min}}$ ($K_{P\,u,u}$)	$\dfrac{AUC_{brain\,0\text{-}90min}/f_{u(brain)}\,V_{u(brain)}}{AUC_{plasma\,0\text{-}90min}/f_{u(plasma)}}$ ($K_{P\,u,u}$)
[11C]Caffeine	micro	2.8	3.0	1.8	0.96[a]	0.52[b]	1.92[c]	0.75	0.4	0.4
	2.5	2.8	2.9	1.8	0.96[a]			0.76	0.4	0.4
[11C]Citalopram	micro	2.2	2.0	48	0.49	0.03[b]	60[d]	11.7	0.7	0.4
	3	3.3	3.0	28.5	0.52			11.7	0.7	0.4
[11C]Clomipramine	micro	3.8	3.4	42	0.01	0.006[e]	863[d]	20.1	12.1	2.3
	0.8	6.2	5.5	22.5	0.01			20.7	12.4	2.4
[11C]Clozapine	micro	5.3	3.5	66	0.09	0.009[b]	220[c]	11.9	1.2	0.6
	1.5	5.2	3.4	19.5	0.11			9.6	0.8	0.4
[11C]Diazepam	micro	3.4	3.9	1.8	0.16	0.05[b]	20[f]	2.0	0.6	0.6
	2	3.4	3.9	1.8	0.12			1.7	0.7	0.7
[11C]Doxepin	micro	4.6	4.8	48	0.14	0.025[g]	115[c]	25.5	4.5	1.6
	0.1	4.1	4.3	19.5	0.14			20.9	3.7	1.3
[11C]Morphine	micro	0.11	0.070	84	0.76	0.5[b]	3.7[f]	0.36	0.2	0.1
	0.5	0.089	0.063	66	0.69			0.19	0.1	0.1
[11C]Nicotine	micro	5.9	4.2	3.5	0.96	1[h]	2.6[c]	5.5	5.7	2.2
	0.12	5.5	3.9	4.5	0.99			6.3	6.6	2.4
[11C]Selegiline	micro	3.3	3.4	4.5	0.14	0.056[b]	38.56[d]	11.2	4.5	2.1
	0.5	4.1	4.3	2.5	0.18			5.9	1.8	0.9
[11C]Sertraline	micro	4.4	5.0	84	0.01	0.00066[b]	4184[d]	24.6	1.6	0.6
	1	4.5	5.1	78	0.02			25.5	0.8	0.3
[11C]Sulpiride	micro	0.0086	0.0075	90	0.93	0.63[b]	4.58[c]	0.0029	0.001	0.0
	2	0.0099	0.0086	78	0.96			0.0022	0.001	0.0
[11C]Venlafaxine	micro	3.6	2.3	16.5	0.92	0.21[b]	10[c]	8.0	1.5	0.9
	2	4.0	2.6	13.5	0.93			8.3	1.5	0.9
[11C]Verapamil	micro	1.3	1.1	5.5	0.25	0.03[i]	54[d]	3.2	0.4	0.2
	0.3	1.9	1.7	5.5	0.28			2.7	0.3	0.2

The unbound fraction in plasma was determined using ultrafiltration on the day of the experiment, whereas the unbound fraction in brain obtained from homogenate ($f_{u,brain}$) or brain slice ($V_{u,brain}$) incubations was obtained from the literature. For the drugs for which $V_{u,brain}$ was not reported in the literature, the pH partition model described by Fridén et al. was used to calculate $V_{u,brain}$ from $f_{u,brain}$.

[a]The unbound fraction in rhesus plasma could not be determined, instead the corresponding free fraction from cynomolgus monkey was used.

[b]Maurer et al., 2005.

[c]Calculated using the pH partition model.

[d]Fridén et al., 2011.

[e]Di et al., 2011.

[f]Fridén et al., 2014.

[g]Summerfield et al., 2007.

[h]Rollema et al., 2010.

[i]Kalvass et al., 2007.

Table 3. Pharmacokinetic Parameters for Intravenously Injected Microdoses of ^{11}C-Labeled Drugs in Rhesus Monkeys

Drug	Dose (mg/kg)	K_1	k_2	V_T	$V_T f_{u(brain)}/f_{u(plasma)}$ ($K_{p\,u,u}$, mL cm^{-3})[a]	$V_T /f_{u(plasma)}V_{u(brain)}$ ($K_{p\,u,u}$, mL cm^{-3})[b]	Preferred Model
[^{11}C]Caffeine	micro	0.22	0.42	0.77	0.42[c]	0.42[c]	2TC
	2.5	0.23	0.38	0.80	0.43[c]	0.43[c]	2TC
[^{11}C]Citalopram	micro	0.40	0.03	21.6	1.32	0.73	2TC
	3	0.35	0.02	17.4	1.00	0.56	1TC
[^{11}C]Clomipramine	micro	0.41	0.01	41.8	25.08	4.84	1TC
	0.8	0.43	0.01	35.4	21.24	4.10	1TC
[^{11}C]Clozapine	micro	0.47	0.09	16.5	1.65	0.83	2TC
	1.5	0.33	0.03	13.0	1.06	0.54	1TC
[^{11}C]Diazepam	micro	0.25	0.28	2.6	0.81	0.81	2TC
	2	0.25	0.27	1.8	0.75	0.75	2TC
[^{11}C]Doxepin	micro	0.86	0.08	46	8.21	2.75	2TC
	0.1	0.70	0.02	29.1	5.20	1.81	1TC
[^{11}C]Morphine	micro	NA	NA	NA	NA	NA	NA[d]
	0.5	NA	NA	NA	NA	NA	NA[d]
[^{11}C]Nicotine	micro	0.66	0.25	8.4	8.75	3.37	2TC
	0.12	0.43	0.14	8.8	8.89	3.42	2TC
[^{11}C]Selegiline	micro	0.30	0.09	NA	NA	NA	NA[e]
	0.5	0.33	0.10	12.2	3.80	1.76	2TC
[^{11}C]Sertraline	micro	0.49	0.007	68.4	4.51	1.63	1TC
	1	0.54	0.008	66.0	2.18	0.79	1TC
[^{11}C]Sulpiride	micro	NA	NA	NA	NA	NA	NA[d]
	2	NA	NA	NA	NA	NA	NA[d]
[^{11}C]Venlafaxine	micro	0.35	0.05	10.3	2.35	1.12	2TC
	2	0.38	0.07	11.4	2.57	1.23	2TC
[^{11}C]Verapamil	micro	0.18	0.08	6.5	0.78	0.48	2TC
	0.3	0.18	0.08	2.8	0.30	0.19	2TC

Rate constants and distribution volumes were calculated for cerebellum. Micro – a microdose lower than one microgram per kg.

[a]$K_{p\,u,u}$ estimated using the free fraction in brain determined by homogenate binding ($f_{u(brain)}$).

[b]$K_{p\,u,u}$ estimated using the free fraction in brain determined by brain slice binding ($V_{u(brain)}$).

[c]The free fraction in cynomolgus monkey plasma was used.

[d]The compartment model did not converge.

[e]Calculated using the 2TC model with irreversible binding to the second compartment.

commercially available CNS drugs. Several approaches for PET data analysis were undertaken to investigate the most relevant outcome parameters that may be obtained from a brain PET measurement. The parameters and some important methodological considerations will be discussed in the following.

C_{max}

Brain radioactivity, expressed as %ID or SUV units ($C_{max,\,\%ID}$ or $C_{max,\,SUV}$), at T_{max} after intravenous injection of a radioligand is a commonly reported parameter in the literature. It can be derived in a straightforward manner from time-activity curves and is thus attractive as a means to differentiate among for the short-listed molecules prior to drug candidate selection. However, this approach has some limitations. First, a valid C_{max} for brain may be obtained only after subtraction of radioactivity in vascular blood. In the present study, this was exemplified by the overestimation of the C_{max} of sulpiride by 2 orders of magnitude when such a correction was omitted. Second, due to the short acquisition time for PET studies, the C_{max} in brain may not necessarily reflect steady-state across the BBB. It is also important to note that all drugs in this study were given intravenously, whereas most CNS drugs are developed for oral administration. The third consideration is related to the inherent inability of PET to distinguish between free and nonspecifically bound drug in brain tissue. The high C_{max} values obtained for clomipramine and sertraline (Figure 2; supplementary Table 3), both having very high nonspecific binding in vitro (supplementary Table 2), may thus

likely reflect high nonspecific binding in vivo rather than high concentrations of free drug in brain. It can be concluded that though brain radioactivity, expressed as $C_{max,\,\%ID}$ or $C_{max,\,SUV}$ at T_{max} are commonly reported parameters they have to be interpreted with caution.

There was a several-fold difference in the observed C_{max} values for the investigated drugs. As anticipated, a low $C_{max,\%ID}$ was obtained for verapamil (~1%ID), which is a known PgP substrate (Qian and Beck, 1990). However, low $C_{max,\%ID}$ values were also observed for morphine and sulpiride (~0.1%ID), of which only the former has been reported to be a PgP substrate (Xie et al., 1999). The $C_{max,\%ID}$ for clomipramine and sertraline together with nicotine was at the higher end. The weight of the human brain corresponds to about 2% of the total body weight. A preferential distribution to brain tissue could tentatively be defined as a $C_{max,\%ID}$ >2% in humans or slightly less for adult cynomolgus or rhesus monkeys. In industrial projects, a $C_{max,\%ID}$ >2% could effectively be used to de-risk molecules in the development phase, although the examples with sulpiride and morphine illustrate that some caution must be exercised before discarding molecules that demonstrate lower brain exposure. Another reason for exercising caution is that the current study was conducted with a limited set of reference drugs and on a limited number of animals.

Partition Coefficients between Brain and Plasma

The arguably most relevant outcome parameter from a PET measurement in relation to brain exposure is the partition
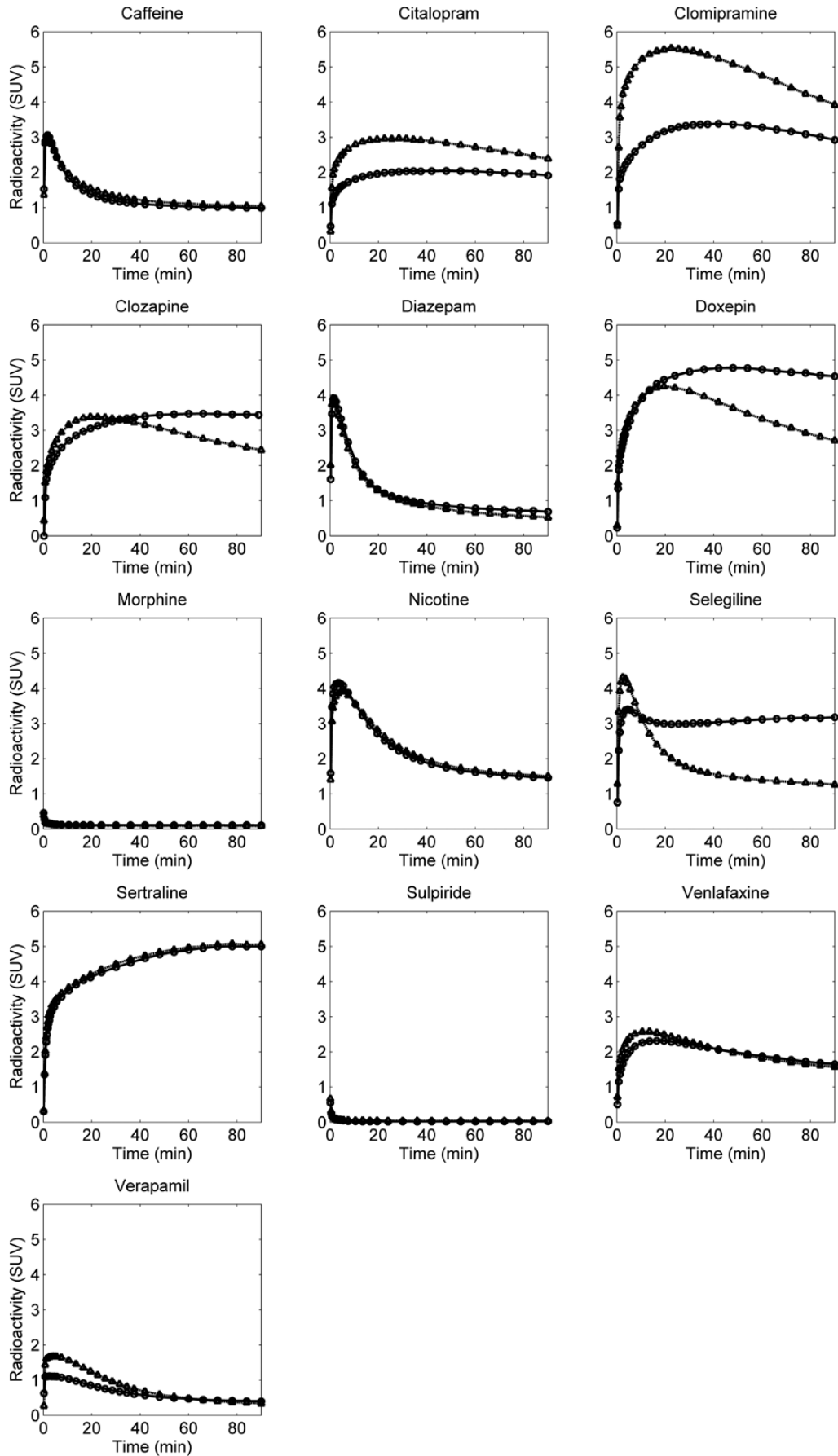
Figure 4. Time curves for brain radioactivity after administration 11C-labeled drugs in rhesus monkeys at microdosing (circles) and pharmacological dosing conditions (triangles). Values are not corrected for radioactivity in cerebral blood.

coefficient between brain and plasma, commonly referred to as K_p in drug development and V_T in the PET imaging community. This ratio is useful, since it can be applied to predict the concentration of a drug in brain based on its concentration in plasma. In the present study, 2 methods were applied to estimate K_p. The first approach comprised dividing the AUCs for time-radioactivity curves for brain and plasma, whereas the second was more elaborate as it comprised a compartmental analysis of the PET data (Table 3). In this case, K_p was calculated from the rate constants that were obtained from the compartmental analysis (supplementary Figure 1). In the present study, lower K_p-values were systematically obtained using the AUC approach. This difference is likely associated with the data acquisition time that probably is not sufficient to assure steady-state conditions. The compartmental analysis is not dependent on steady-state conditions to identify the critical rate constants across the BBB, although the reliability of the single rate constants may not be excellent for short acquisition times. It is important to emphasize that the most accurate analysis is expected to be based on a compartmental analysis.

The partition coefficient, K_p, for the 13 drugs examined in the present study varied greatly. A common view in drug discovery and development is that high nonspecific binding in brain leads to high K_p. This view was supported by the observation that the 2 drugs having the highest levels of nonspecific binding in brain tissue in vitro, sertraline and clomipramine ($V_{u,brain}$-values of 4184 and 863, respectively), also had the highest K_p. An advantage of combining the free fraction from in vitro experiments, that is, $f_{u,brain}$ or $V_{u,brain}$, with K_p measured by PET is that the free concentration in brain in vivo can be estimated. After correcting for nonspecific binding in brain and plasma, the unbound partition coefficient ($K_{p.uu}$) for 8 of the 12 CNS drugs approached unity (within 3-fold), suggesting that the passage across the BBB can be characterized as passive diffusion. Of the remaining drugs, verapamil, morphine, and sulpiride had a $K_{p.uu}$ value well below unity, which may indicate impaired diffusion over the BBB or active efflux. Indeed, both morphine and verapamil are known PgP-substrates (Qian and Beck, 1990; Xie et al., 1999), whereas sulpiride has been shown to have low permeability (Maurer et al., 2005). The high $K_{p.uu}$ for the last 2 deviant drugs, nicotine and clomipramine, would imply active transport over the BBB. However, since no active transport mechanism has been reported for either of these drugs, other explanations are more likely. For clomipramine, the very high plasma protein binding (99.9%) introduces an uncertainty, since small errors in the measurement of this variable have a large impact on $K_{p.uu}$. Though other methods may be more appropriate for the determination of free drug in plasma, ultrafiltration is the only technique compatible with the short half-life of carbon-11. Another source of error is related to the inability of PET to distinguish between radiochemical entities. This consideration applies to clomipramine and nicotine forming pharmacologically active metabolites that have been shown to readily cross the BBB (Gex-Fabry et al., 2000; Hukkanen et al., 2005). Radioactive metabolites in brain may thus contribute to the relatively high $K_{p.uu}$-values obtained for these drugs.

A critical condition for the estimation of $K_{p.uu}$ is the validity of the method used in vitro for determination of free fraction in brain. Of the 2 methods currently used in drug discovery, namely homogenate ($f_{u(brain)}$) and brain slice binding ($V_{u(brain)}$), the latter has been proposed as more relevant for in vivo conditions, since it not only accounts for nonspecific binding in brain tissue but also for the overall intracellular disposition of a drug (Friden et al., 2011). In support of the proposed superior validity of $V_{u(brain)}$,

a $K_{p.uu}$ close to unity was obtained for 6 of the 13 drugs when $V_{u(brain)}$ was applied (Table 3), whereas the same was observed for only 2 of the drugs (citalopram and clozapine) when $f_{u(brain)}$ was applied. For the remaining drugs, there was either no difference because of the absence of cationic functional groups (caffeine, diazepam), an active efflux process, or impaired permeability that would confound such a comparison (morphine, sulpiride, verapamil).

The application of $V_{u(brain)}$ values, obtained from rat brain slices, to estimate $K_{p.uu}$ in nonhuman primates is based on the assumption that there are no significant species differences. Though there are no studies on species differences in $V_{u(brain)}$, it has been shown that the parameter can be fully explained by the species-indifferent $f_{u(brain)}$ variable and intracellular pH partitioning (Friden et al., 2011). Hence, if pH partitioning is conserved across species, which is not unreasonable considering that it is a basic intracellular process, $V_{u(brain)}$ would also be species independent. However, this independency requires further empirical confirmation.

Compartmental Analysis

The observation that the 2-tissue compartment model was preferred for most of the investigated drugs may suggest the presence of specific binding compartment in brain. However, since pharmacological dosing had a limited saturating effect on the binding in brain for most compounds, an additional interpretation would be distribution into an intracellular compartment or a kinetically distinguishable nonspecific binding compartment (Farde et al., 1998). Worth noting is that for some of the drugs with very high nonspecific binding in vitro, for example, clomipramine and sertraline, the 1-tissue compartment model was sufficient to describe the data. This observation may imply that the nonspecifically bound compartment is seen by the model as dominant.

Brain Exposure at Microdosing Conditions vs Pharmacological Dosing Conditions

The brain exposure at microdosing and therapeutically relevant conditions was generally in good agreement, and on average there was not more than a 1.5-fold difference in any of the parameters measured in the 2 conditions. The presence of saturable binding or transport, which were identified as potential confounders a priori, did not greatly affect the average outcome parameters for the drugs investigated in this study with the exception for seligiline, for which a 2-fold reduction in the ratio between AUC in brain and plasma was observed. However, some observations were made and will be discussed in the following.

For most drugs, a modest reduction in K_p was observed as a result of pharmacological dosing. This observation is most likely explained by the presence of saturable receptor binding in brain. In support of this hypothesis, the most pronounced effect of pharmacological dosing was observed for doxepin and seligiline, 2 drugs that have been successfully applied as PET radioligands owing to their high affinity for the H1-histamine receptor and MAO-B in brain, respectively (Fowler et al., 1987; Mochizuki et al., 2004). Although this is not expected to be the rule, the observation with these 2 drugs illustrates the importance of performing measurements at pharmacological dosing conditions to avoid a potential overestimatation of K_p when based on microdosing conditions.

Increased peak brain concentrations following pharmacological dosing conditions is well documented in the literature for

PET radioligands and often attributed to saturation of peripheral binding sites. An illustrative example of this phenomenon was reported by Suhara et al. (1998), who observed a reservoir of cyanoimipramine in lungs that could be displaced after administration of a pharmacological dose of clomipramine. In this study, the modest increase in C_{max} observed for many of the drugs is likely explained by such saturation, since plasma protein binding was not affected to a noteworthy degree between the 2 conditions.

Drug Metabolism

The rate of drug metabolism under microdosing and pharmacological dosing conditions was remarkably similar for all investigated drugs. It is anticipated that higher drug doses would lead to saturation of cytochrome P enzymes, but this was not observed for the dose range investigated in this study. Thus, in addition to providing an in vivo measurement of brain exposure, a PET microdosing study may also shed further light on the nature and extent of drug metabolism. A noteworthy observation from the study of radioactive metabolites in plasma was the very rapid degradation of morphine, which represented only 4% of the total radioactivity in plasma at 45 minutes. The rapid turnover of morphine is well known as is the formation of 2 pharmacologically active glucoronide metabolites that are transported across the BBB to a similar extent as morphine and thus contribute to the overall drug effect (Shimomura et al., 1971).

Conclusions

This study represents the largest examination of the brain exposure of commercially available CNS drugs using PET microdosing. For 10 of the 12 CNS drugs, the C_{max} calculated as percent of injected dose was >2 %, thus supporting a preferential distribution to brain. The results corroborate the view that PET-microdosing has an important role in drug development, preferably at an early stage and in combination with traditional PK parameters.

Acknowledgments

Statement of Interest

References

Akaike H (1992) [Data analysis by statistical models]. No To Hattatsu 24:127–133.

Arrowsmith J (2011) Trial watch: Pphase II failures: 2008-2010. Nat Rev Drug Discov 10:328–329.

Bergstrom M, Grahnen A, Langstrom B (2003) Positron emission tomography microdosing: a new concept with application in tracer and early clinical drug development. Eur J Clin Pharmacol 59:357–366.

Di L, Umland JP, Chang G, Huang Y, Lin Z, Scott DO, Troutman MD, Liston TE (2011) Species independence in brain tissue binding using brain homogenates. Drug Metab Dispos 39:1270–1277.

Farde L, Eriksson L, Blomquist G, Halldin C (1989) Kinetic analysis of central [11C]raclopride binding to D2-dopamine receptors studied by PET--a comparison to the equilibrium analysis. J Cereb Blood Flow Metab 9:696–708.

Farde L, Ito H, Swahn CG, Pike VW, Halldin C (1998) Quantitative analyses of carbonyl-carbon-11-WAY-100635 binding to central 5-hydroxytryptamine-1A receptors in man. J Nucl Med 39:1965–1971.

Fowler JS, MacGregor RR, Wolf AP, Arnett CD, Dewey SL, Schlyer D, Christman D, Logan J, Smith M, Sachs H, et al. (1987) Mapping human brain monoamine oxidase A and B with 11C-labeled suicide inactivators and PET. Science 235:481–485.

Friden M, Bergstrom F, Wan H, Rehngren M, Ahlin G, Hammarlund-Udenaes M, Bredberg U (2011) Measurement of unbound drug exposure in brain: modeling of pH partitioning explains diverging results between the brain slice and brain homogenate methods. Drug Metab Dispos 39:353–362.

Friden M, Wennerberg M, Antonsson M, Sandberg-Ställ M, Farde L, Schou M (2014) Identification of positron emission tomography (PET) tracer candidates by prediction of the target-bound fraction in the brain. EJNMMI Res 4:50.

Gex-Fabry M, Haffen E, Paintaud G, Bizouard P, Sechter D, Bechtel PR, Balant LP (2000) Population pharmacokinetics of clomipramine, desmethylclomipramine, and hydroxylated metabolites in patients with depression receiving chronic treatment: model evaluation. Ther Drug Monit 22:701–711.

Gunn RN, Summerfield SG, Salinas CA, Read KD, Guo Q, Searle GE, Parker CA, Jeffrey P, Laruelle M (2012) Combining PET biodistribution and equilibrium dialysis assays to assess the free brain concentration and BBB transport of CNS drugs. J Cereb Blood Flow Metab 32:874–883.

Halldin C, Gulyas B, Farde L (2001) PET studies with carbon-11 radioligands in neuropsychopharmacological drug development. Current Pharmaceutical Design 7:1907–1929.

Huang SC, Feng DG, Phelps ME (1986) Model dependency and estimation reliability in measurement of cerebral oxygen utilization rate with oxygen-15 and dynamic positron emission tomography. J Cereb Blood Flow Metab 6:105–119.

Hukkanen J, Jacob P, 3rd, Benowitz NL (2005) Metabolism and disposition kinetics of nicotine. Pharmacol Rev 57:79–115.

Innis RB, Carson R (2007) Consensus nomenclature: its time has come. Eur J Nucl Med Mol Imaging 34:1239.

Kalvass JC, Maurer TS, Pollack GM (2007) Use of plasma and brain unbound fractions to assess the extent of brain distribution of 34 drugs: comparison of unbound concentration ratios to in vivo p-glycoprotein efflux ratios. Drug Metab Dispos 35:660–666.

Karlsson P, Farde L, Halldin C, Swahn CG, Sedvall G, Foged C, Hansen KT, Skrumsager B (1993) PET examination of [11C]NNC 687 and [11C]NNC 756 as new radioligands for the D1-dopamine receptor. Psychopharmacology (Berl) 113:149–156.

Kola I, Landis J (2004) Can the pharmaceutical industry reduce attrition rates? Nat Rev Drug Discov 3:711–715.

Lammertsma AA, Bench CJ, Price GW, Cremer JE, Luthra SK, Turton D, Wood ND, Frackowiak RS (1991) Measurement of cerebral monoamine oxidase B activity using L-[11C]deprenyl and dynamic positron emission tomography. J Cereb Blood Flow Metab 11:545–556.

Lappin G (2010) Microdosing: current and the future. Bioanalysis 2:509–517.

Lee CM, Farde L (2006) Using positron emission tomography to facilitate CNS drug development. Trends Pharmacol Sci 27:310–316.

Leenders KL, Perani D, Lammertsma AA, Heather JD, Buckingham P, Healy MJ, Gibbs JM, Wise RJ, Hatazawa J, Herold S, et al. (1990) Cerebral blood flow, blood volume and oxygen utilization. Normal values and effect of age. Brain 113:27–47.

Maurer TS, Debartolo DB, Tess DA, Scott DO (2005) Relationship between exposure and nonspecific binding of thirty-three central nervous system drugs in mice. Drug Metab Dispos 33:175–181.

Mintun MA, Raichle ME, Kilbourn MR, Wooten GF, Welch MJ (1984) A quantitative model for the in vivo assessment of drug binding sites with positron emission tomography. Ann Neurol 15:217–227.

Mochizuki H, Kimura Y, Ishii K, Oda K, Sasaki T, Tashiro M, Yanai K, Ishiwata K (2004) Simplified PET measurement for evaluating histamine H1 receptors in human brains using [11C]doxepin. Nucl Med Biol 31:1005–1011.

Osman S, Lundkvist C, Pike VW, Halldin C, McCarron JA, Swahn CG, Farde L, Ginovart N, Luthra SK, Gunn RN, Bench CJ, Sargent PA, Grasby PM (1998) Characterisation of the appearance of radioactive metabolites in monkey and human plasma from the 5-HT1A receptor radioligand, [carbonyl-11C]WAY-100635--explanation of high signal contrast in PET and an aid to biomathematical modelling. Nucl Med Biol 25:215–223.

Qian XD, Beck WT (1990) Binding of an optically pure photoaffinity analogue of verapamil, LU-49888, to P-glycoprotein from multidrug-resistant human leukemic cell lines. Cancer Res 50:1132–1137.

Rollema H, Shrikhande A, Ward KM, Tingley FD, 3rd, Coe JW, O'Neill BT, Tseng E, Wang EQ, Mather RJ, Hurst RS, Williams KE, de Vries M, Cremers T, Bertrand S, Bertrand D (2010) Preclinical properties of the alpha4beta2 nicotinic acetylcholine receptor partial agonists varenicline, cytisine and dianicline translate to clinical efficacy for nicotine dependence. Br J Pharmacol 160:334–345.

Shimomura K, Kamata O, Ueki S, Ida S, Oguri K (1971) Analgesic effect of morphine glucuronides. Tohoku J Exp Med 105:45–52.

Suhara T, Sudo Y, Yoshida K, Okubo Y, Fukuda H, Obata T, Yoshikawa K, Suzuki K, Sasaki Y (1998) Lung as reservoir for antidepressants in pharmacokinetic drug interactions. Lancet 351:332–335.

Summerfield SG, Read K, Begley DJ, Obradovic T, Hidalgo IJ, Coggon S, Lewis AV, Porter RA, Jeffrey P (2007) Central nervous system drug disposition: the relationship between in situ brain permeability and brain free fraction. J Pharmacol Exp Ther 322:205–213.

Varrone A, Sjoholm N, Eriksson L, Gulyas B, Halldin C, Farde L (2009) Advancement in PET quantification using 3D-OP-OSEM point spread function reconstruction with the HRRT. Eur J Nucl Med Mol Imaging 36:1639–1650.

Wong DF, Wagner HN Jr, Tune LE, Dannals RF, Pearlson GD, Links JM, Tamminga CA, Broussolle EP, Ravert HT, Wilson AA, Toung JK, Malat J, Williams JA, O'Tuama LA, Snyder SH, Kuhar MJ, Gjedde A (1986) Positron emission tomography reveals elevated D2 dopamine receptors in drug-naive schizophrenics. Science 234:1558–1563.

Xie R, Hammarlund-Udenaes M, de Boer AG, de Lange EC (1999) The role of P-glycoprotein in blood-brain barrier transport of morphine: transcortical microdialysis studies in mdr1a (-/-) and mdr1a (+/+) mice. Br J Pharmacol 128:563–568.